

# IETR and TKK- MilliLab measurements cooperation in ACE 2 context : characterization of a Half Maxwell Fish Eye lens at 110 and 150 GHz

*L. Le Coq<sup>(1)</sup>, M. Vaaja<sup>(2)</sup>, B. Fuchs, O. Lafond<sup>(1)</sup>, J. Ala Laurinaho<sup>(2)</sup>,  
J. Mallat<sup>(2)</sup>, M. Himdi<sup>(1)</sup>, A. V. Räsänen<sup>(2)</sup>*

<sup>1</sup>IETR, University of Rennes 1, France,  
laurent.le-coq@univ-rennes1.fr

<sup>2</sup>MilliLab, SMARAD, Dept. of Radio Science and Engineering, TKK Helsinki University of  
Technology, Finland

## Introduction

During ACE 2, transversal actions between activities were promoted. In such a context, and due to their research interests, TKK and IETR decided to cooperate for measuring a lens in millimetric bands. This lens, a Half Maxwell Fish Eye structure fed by an open ended waveguide, has been designed in an IETR PhD-study for applications in the W-band. Due to IETR measurement facilities frequency limitations, no measurements could be performed above 110 GHz. Then, in the ACE 2 context, measurements were planned with TKK to characterize this lens at 110 GHz and 150 GHz. The 110 GHz frequency was chosen for two main reasons: to check lens capabilities with a WR-6 open ended waveguide as a feed, using IETR antenna test facility; and to make comparisons between IETR far-field antenna test range and TKK planar near-field antenna test range results. Presented measurements were performed in IETR in May 2008 and in TKK in June 2008.

## Half Maxwell Fish Eye lens

The antenna under test is a Half Maxwell Fish Eye (HMFE) lens fed by an open ended waveguide. The diameter of the lens is 60 mm. This structure (Fig. 1) was designed for applications in the W-band [1-2]. Characterization was performed in this band in order to check specific software development and radiating capabilities (Fig. 2).



Fig. 1 : Prototype top and side view

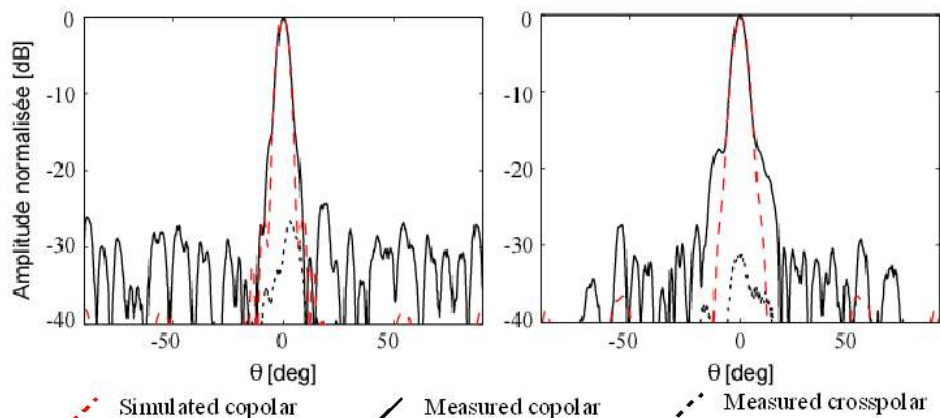


Fig. 2 : 75 GHz results in E- (left) and H-plane (right)

Due to its capabilities [1-3], characterization of the HMFE at highest frequencies is of main interest for next automotive radar generation for example. Even though the actual prototype is not dimensioned for frequencies higher than 110 GHz, measurements at 150 GHz should give more information on: potentiality of such structure at highest frequencies; problem of feed positioning; and realization errors on radiating characteristics.

#### Characterization at 110 GHz and 150 GHz

IETR antenna test facilities are actually limited in frequency at 110 GHz. In order to proceed to 150 GHz characterization, cooperation has been established between IETR and TKK-MilliLab in the ACE 2 context. The roadmap is as follows: IETR modification of the radiating structure to use a WR6 open ended waveguide as a feed; characterisation of the new radiating structure in IETR antenna test facility at 110 GHz for the first verification; characterization at 110 GHz and 150 GHz by TKK-MilliLab.

First measurements are performed at 110GHz for two main reasons: to check the use of a WR-6 open ended waveguide as a feed and to have a common frequency for comparisons between IETR and TKK-MilliLab results. In fact, for travel, the prototype is partially dismantled and the first measurements in TKK-MilliLab must be used to check the rebuilt antenna.

The TKK-MilliLab measurement facility has a planar near-field scanner made by Near-field Systems (NSI). The scanner has a moving range of about  $1.5 \text{ m} \times 1.5 \text{ m}$ . The RF-instrumentation is based on AB Millimetre MVNA 8-350 Vector Network Analyzer, which enables vector measurements. Vector measurements are needed in order to process the near-field data to far-field. In all near-field scans, the scanning area is  $240 \text{ mm} \times 240 \text{ mm}$ . The scanning steps are 1.5 mm and 1 mm in both directions at 110 GHz and 150 GHz, respectively.

#### Comparison at 110 GHz :

Figure 3 shows the far-field results transformed from the near-field data. A low-level MVNA reference signal leakage causes an effect, which is analogous to a constant phase square aperture antenna and the resulting cross-shaped far-field pattern is superpositioned on the AUT antenna pattern. The level of the spurious is quite high as the rectangular scan area aperture is larger than the lens antenna aperture and the leakage energy is summed in the far-field transformation causing a large error signal in the direction perpendicular to the scanning plane. This is clearly seen in the cross-polar result. Also, in the co-polar result the artefact is seen and the level of the artefact is 5.5 dB lower than the co-polar peak.

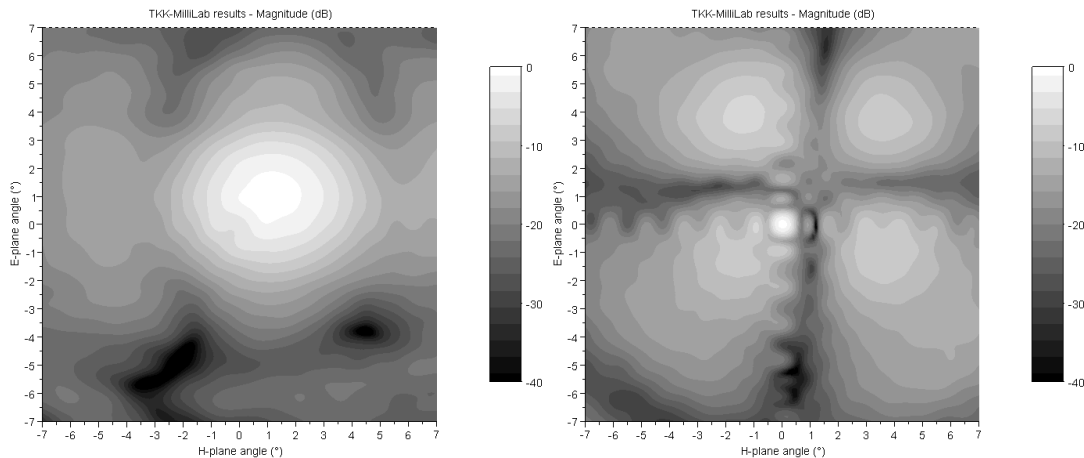


Fig. 3 : Co-polar and cross-polar measurement results at 110 GHz: far-field transformed from the uncompensated near-field data.

The spurious leakage signal is compensated in the results of Figs. 4 and 5. The compensation is accomplished by choosing a small corner part of the near-field data to sample the noise level. The actual antenna signal is not significant anymore and the leakage signal is dominant. An average of the field in the corner points gives the constant leakage signal value and it is removed from the near-field data. In all compensations in this paper,  $20 \times 20$  corner points are used in the average calculation. After removing the constant term from all the near-field data points, the normal near-field to far-field transformation including probe compensation is carried out.

The leakage signal compensation could be done also by measuring the leakage with the transmitter terminated and then subtracting the result from the uncompensated near-field data.

IETR and TKK-MilliLab measurements at 110 GHz show good agreements (Figs. 4 and 5). The presented results in Fig. 4 show a 2D map of the normalized co-polar pattern limited on the area of interest  $[-7:7]^\circ$  for E- and H-plane angles (Fig. 4), focusing on the representation of the main beam. In both case, a small tilt can be noticed due to misalignment between the lens and the feed. The first nulls are partially filled and the first side lobes are merged with the main beam in the H-plane and are an expression of lens realization uncertainties. The main lobe location is shifted between the two measurements sets:  $0,3^\circ$  for the H-plane angles and  $0,2^\circ$  for the E-plane angles.

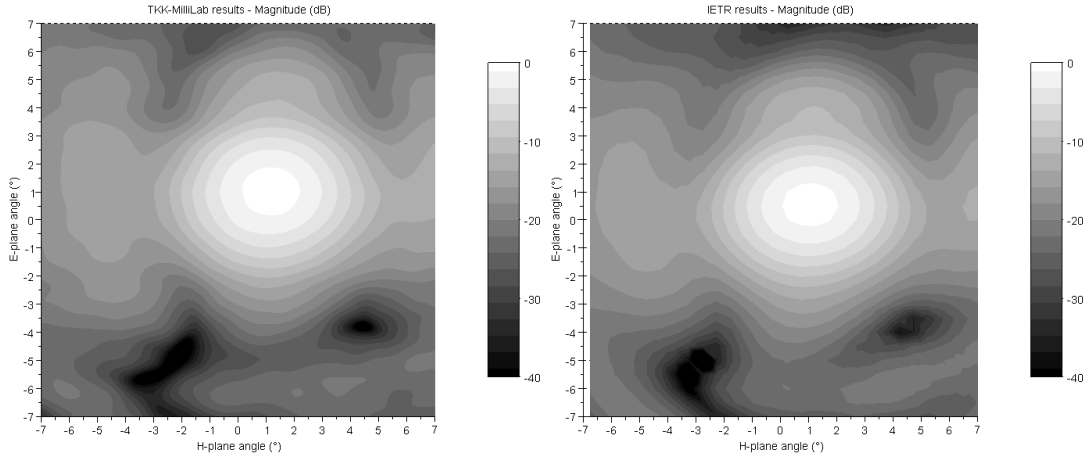


Fig. 4 : Co-polar measurements results at 110 GHz.

Figure 5 shows the cross-polar patterns at the same angular range as the co-polar patterns. Slight angular shift is observed as in the co-polar results.

Discrepancies and angle shift between the two measurements sets (Fig. 4 and 5) can be induced by the small differences between prototype measured in IETR and its rebuilt version measured in TKK-MilliLab. In fact, due to the mounting structure architecture, the position of the lens could not be insured with enough precision to avoid small rotation of the lens in the feed coordinate system when the prototype is dismantled and remounted. The result is a small shift of the main beam location.

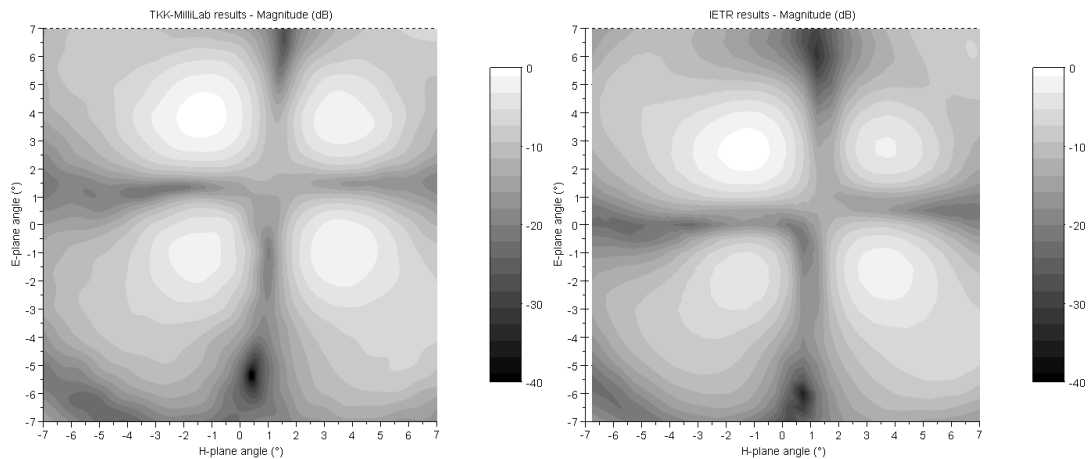


Fig. 5 : Cross-polar measurements results at 110 GHz.

Using classical representations of co-polar in E- and H-planes (Fig. 6 and 7) of the main lobe, we can see that the two measurements sets are very similar: lobes positions and levels are coherent, and half power beam widths are in E-plane  $2.98^\circ$  and  $3.00^\circ$ , and in H-plane  $3.45^\circ$  and  $3.57^\circ$  for IETR and TKK-MilliLab results respectively.

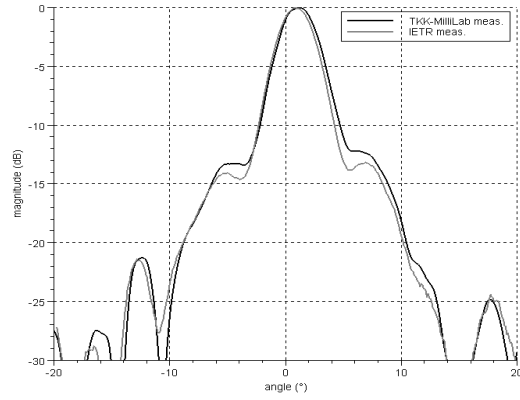
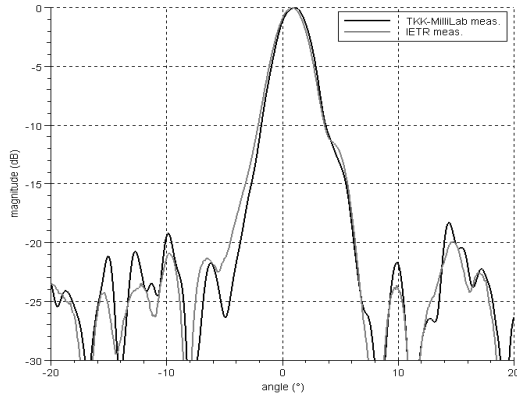


Fig. 6 : E-plane Co-polar comparison at 110 GHz. Fig. 7 : H-plane Co-polar comparison at 110 GHz.

**150 GHz results**

Results at 150 GHz (Figs. 8 and 9) also show a tilt of the main beam and an increase of the first side lobes in the H-plane due to lens structure errors. The leakage error is compensated as in the 110 GHz results. In the cross-polar results, there is a residual of the leakage artefact, which is not compensated properly with the technique used here.

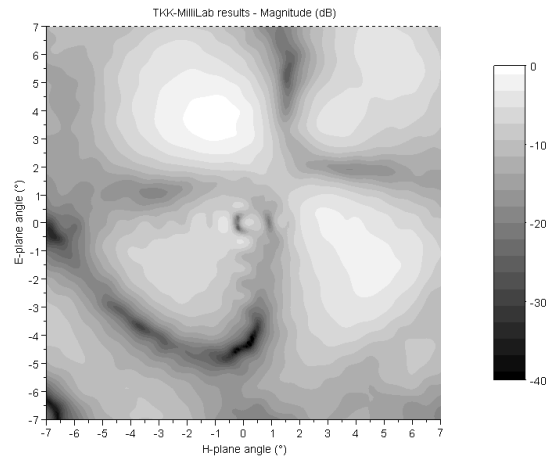
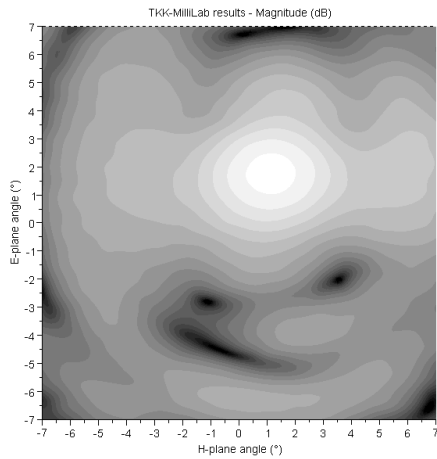


Fig. 8 : Normalized compensated co-polar results at 150 GHz.

Fig. 9 : Normalized compensated cross-polar results at 150 GHz.

Figs. 10 and 11 show the uncompensated results at 150 GHz. The bright spot is 4.3 dB higher than the antenna co-polar pattern peak. In the cross-polar pattern, the artefact is very large compared to the desired antenna pattern.

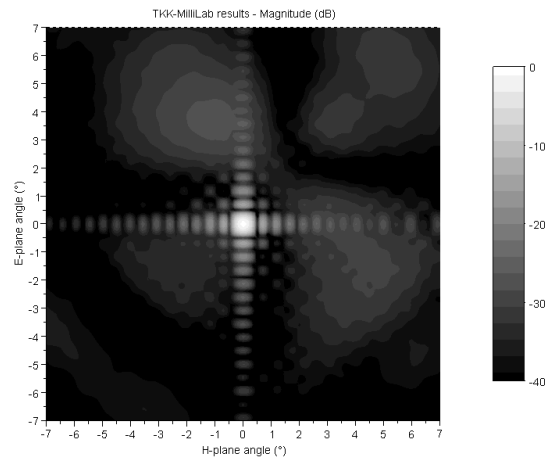
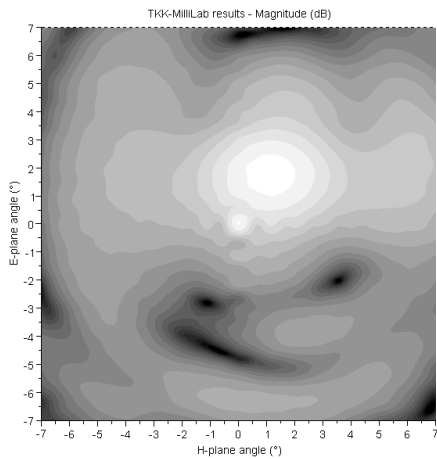


Fig. 10 : Normalized uncompensated co-polar results at 150 GHz.

Fig. 11 : Normalized uncompensated cross-polar results at 150 GHz.

### **Conclusion**

Thanks to ACE 2 umbrella, measurement cooperation between IETR and TKK-MilliLab has been established and thus enabling characterization of a half Maxwell Fish Eye lens at 150 GHz. Results at 110 GHz provide comparison between IETR and TKK-MilliLab antenna test facilities. The agreement between the results is very good. Results at 150 GHz provide the first information for future development of such lens in the G-band.

### **References**

- [1] B. Fuchs, O. Lafond, S. Rondineau and M. Himdi, "Design and characterization of half Maxwell fish-eye lens antennas in millimeter waves," IEEE Trans. Microwave Theory Tech., vol. 54, no. 6, pp. 2292-2300, June 2006.
- [2] B. Fuchs, L. Le Coq, O. Lafond, S. Rondineau, M. Himdi : ' Design optimization of multishell Luneburg lenses', IEEE Transactions on Antennas and Propagation, vol. 55, n°2, pp. 283-289, Feb 2007.
- [3] French Patent n° 2888407 (2007): O. Lafond, M. Himdi, S. Rondineau, B. Fuchs : 'Lentilles inhomogènes à gradient d'indice de type œil de Poisson de Maxwell, système d'antennes et applications correspondantes'.